# Realization of a quantum walk in phase space using resonator-assisted double quantum dots

Zhihao Bian, Hao Qin, Xiang Zhan, and Rong Zhang
*Department of Physics, Southeast University, Nanjing 211189, China*

Peng Xue*
*Department of Physics, Southeast University, Nanjing 211189, China and*
*State Key Laboratory of Precision Spectroscopy, East China Normal University, Shanghai 200062, China*

(Dated: July 31, 2014)

We implement a quantum walk in phase space with a new mechanism based on the superconducting resonator-assisted double quantum dots. By analyzing the hybrid system, we obtain the necessary factors of realization of a quantum walk in phase space: the walker, coin, coin flipping and conditional phase shift. In order to implement the coin flipping operator, we add a driving field to the resonator. The interaction between the quantum dots and resonator field is used to implement conditional phase shift. Furthermore, we show with different driving fields the quantum walk in phase space exhibits a ballistic behavior over 25 steps and numerically analyze the factors which influence the spreading of the walker in phase space.

Key words: quantum walk, superconducting circuit QED, quantum-to-classical transmission, decoherence

PACS numbers: 03.67.Ac, 42.50.Pq, 74.50.+r

arXiv:1407.8148v1 [quant-ph] 30 Jul 2014

## I. INTRODUCTION

Quantum walk (QW) [1–10] is appealing as an intuitively model in quantum computing and quantum algorithms [11–14]. Because it exponentially speeds up the hitting time in glued tree graphs. Furthermore, QW offers a quadratic gain over classical algorithms on account of the diffusion spread (standard deviation), which is proportional to elapsed time $t$, rather than $\sqrt{t}$ for the classical random walk (RW) [15, 16]. Thus, the conception of physical implementation of QW has become important and attract more and more attention. Although realizations of QWs have been proposed in different systems such as trapped ions [17–19], photons [20–30], nuclear magnetic resonance [31, 32] etc., the solid state systems are attractive because of the stability and expected scalability.

Recently, quantum computing with quantum dots has made a huge progress [33–40], and the technique for coupling electrons associated with semiconductor double-dot molecule to a microwave stripline resonator has become more and more matured. Here we make use of the technology and propose the implementation of a one-dimensional QW in phase space with superconducting resonator-assisted quantum double-dot. The walker is presented by a coplanar transmission line resonator with a single mode and a two-level system–one electron shared by double dots via tunneling serves as the quantum coin.

In our scheme the QW is executed with indirect flipping of the coin via directly driving the resonator and allows controllable decoherence over circles in phase space (PS) for observing the transition between QW and RW [41–43]. In next section we give a brief introduction of the QW in PS. In Sec. III, we implement QW via realizing the walker, coin, coin flipping and conditional phase shift. In addition to the numerical analysis under the different driving fields, we we observe the ballistic behavior of QW in PS and the QW-RW transmission with the influence of decoherence introduced by the shift operation in the position space.

## II. BRIEF INTRODUCTION OF QW IN PS

Similar to the QW on a line in position space in which the walker moves towards left or right based on the coin state, for QW on circle in PS, the walker rotates either clockwise or counter-clockwise along the circle in PS by the same amount, say an angle $\Delta\theta$, with the choice of $\pm\Delta\theta$ strictly random through the impulse, which is applied by a harmonic oscillator.

In an ideal QW on a circle, the coin is replaced by a two-level system with internal states $|0\rangle$ and $|1\rangle$. Here we introduce the finite-dimensional orthogonal phase state representation [44]

$$|\theta_k = \frac{2\pi k}{d}\rangle = \frac{1}{\sqrt{d}}\sum_{n}^{d-1} e^{in\theta_k}|n\rangle, k \in Z, \qquad (2.1)$$

where $|n\rangle$ is the Fock state. If the step size $\Delta\theta = 2\pi/d, d \in N$, then the walker always remains on the circle with angular lattice spacing $\Delta\theta$. The walker walks in PS with a state $|\theta_k\rangle$ which can be decomposed into the phase states. We introduce the rotation operator $\hat{R}_m = e^{in\theta_m}, m \in Z$, then we have $\hat{R}_m|\theta_k\rangle = |\theta_{k+m}\rangle$. We

*Electronic address: gnep.eux@gamil.com

choose the Hadamard operator

$$H = \frac{1}{\sqrt{2}}\begin{pmatrix} 1 & 1 \\ 1 & -1 \end{pmatrix} \tag{2.2}$$

as the coin flipping operator and the unitary operation of one step of the QW in PS is given by

$$E = e^{in\sigma_z \Delta\theta} \tag{2.3}$$

with the number operator on the walker state $n = a^\dagger a$, $a^\dagger$ and $a$ are the creation and annihilation operators, respectively. $\sigma_z = \begin{pmatrix} 1 & 0 \\ 0 & -1 \end{pmatrix}$ is one of the Pauli operators applied on the coin.

We define the initial state of walker+coin system as

$$|\phi_0\rangle = |\phi_0\rangle \otimes |\varphi_0\rangle, \tag{2.4}$$

where $|\varphi_0\rangle$ is the initial coin state. After $N$ steps, the system evolves to

$$|\phi_N\rangle = [E(I_w \otimes H)]^N |\phi_0\rangle. \tag{2.5}$$

The walker's phase distribution on a circle is

$$P(\theta) = \langle\theta|\rho_w|\theta\rangle \tag{2.6}$$

with $d$ equally spaced values of $\theta = \theta_k$ and $\rho_w = \mathrm{Tr}_c|\phi_N\rangle\langle\phi_N|$ is the reduced density matrix of the walker after tracing out the coin.

The standard deviation of the phase distribution satisfies, $\sigma$, which is the symbol of the spreading of the QW, is linear on time $t$. Therefore, in sufficiently short time, the relation between phase spreading with time on a circle is a power law and satisfies [42]

$$\ln\sigma = \zeta \ln t + \xi, \tag{2.7}$$

with $\zeta = 1$ for the QW and $\zeta = 1/2$ for the RW.

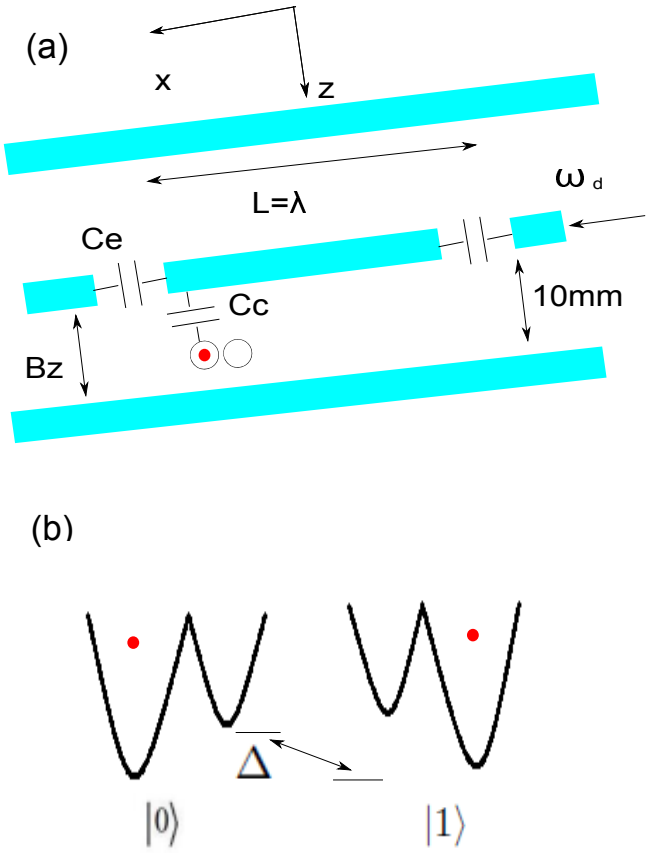


FIG. 1: (Color online.) (a) Experimental proposal for QW with superconducting resonator-assisted quantum double-dot. The red dot stands for the electron. The coupling between the resonator and the double-dot can be switched on and off via the external electric field along the $x$ axis. The superducting resonator is driven by a field along the $x$ axis for implementation of coin flipping. (b) The double-dot modeled as a double-well potential. The basis of the qubit states represent the electron either in the left or right potential via tunneling. The energy difference between the states $|0\rangle$ and $|1\rangle$ is $\Delta$.

## III. PHYSICAL IMPLEMENTATION OF QW

### A. Quantum coin and walker

Circuit Quantum Electrodynamics (QED) is a device which studies the interaction between quantum particles and the quantized electromagnetic modes inside a resonator. In this paper we consider a hybrid QED system of superconducting resonator-assisted quantum double-dot shown in Fig. 1a. One of the dots is capacitively coupled to the resonator, and an electron shared by two adjacent dots coupled via tunneling. The double dots can be modeled as a double-well potential shown in Fig. 1b. Generally, we add an external magnetic field along the axis $z$ to the double dots, which the modest $B_z$ is 100mT [45]. Based on the external magnetic field, there exists an energy difference between the two potentials and the electron can tunnel between the two quantum dots. We define the basis of qubits $|0\rangle$ for the electron appearing in the left dot and $|1\rangle$ for the electron in the right dot. From Fig. 1b we see the energy difference, namely energy cost which moves the electron from the right dot to the left, between the states $|0\rangle$ and $|1\rangle$ is $\Delta = T$, where $T$ is the rate of electron tunneling in the different dots.

After adding the magnetic field to the quantum dots, the double-well potential forms a circuit [46]. We just consider one circumstance whether the electron locates in left dot or right, the Hamiltonian describing the circuit is given by

$$\hat{H}_Q = \sum_{N=0,1} E_c(N-N_g)^2|N\rangle\langle N| - \Delta\left(|N+1\rangle\langle N| + H.C.\right), \tag{3.1}$$

where $E_c = e^2/2C_{tot}$ is the charge energy, $C_{tot} = C_g + C_J$ is the total capacitance in the circuit, $C_J$ is the Josephson capacitance and $C_g$ is voltage biased from a lead hav-

ing capacitance to the circuit. $N_g = C_g V_g/2e$ is the gate charge which stands for the total polarization charge. Restricting the gate charge to the range $N_g \in [0, 1]$ by using the voltage $V_g$, the Hamiltonian in Eq. (3.1) is rewritten as

$$\hat{H}_{\rm Q} = \frac{1}{2}E_c(1-2N_g)\sigma_z - \Delta\sigma_x. \tag{3.2}$$

So far, we show the Hamiltonian of the double-well potential. From Eq. (3.2) we see the double-well potential presenting the double-dot system with effective electric fields along the $x$ and $z$ directions, and the system with internal states $|0\rangle$ and $|1\rangle$ can be used as a two-level quantum coin.

Now we consider the circuit QED of double dots coupled to a superconducting resonator. The dots are located in the center of the resonator. If the oscillator mode of the resonator is coupled to the double-dot, by using the coordinate system transformation $R = \begin{pmatrix} \cos\theta & -\sin\theta \\ \sin\theta & \cos\theta \end{pmatrix}$, and choosing $2N_g = 1$, $\theta = \pi/2$, the Hamiltonian of the interacting qubit and resonator system with the rotating wave approximation takes the form ($\hbar = 1$)

$$\hat{H}_{\rm JC} = \omega_c a^\dagger a + \frac{\Omega}{2}\sigma_z + g(a^\dagger\sigma_- + a\sigma_+), \tag{3.3}$$

where $\omega_c$ is the frequency of the resonator, $\Omega = \sqrt{{E_c}^2(1-2N_g)^2 + 4\Delta^2}$ [47] is the resonator induced energy splitting of the qubit, $g = e\frac{C_g}{C_{\rm tot}}\sqrt{\frac{\omega_c}{L}}$ is the vacuum Rabi frequency. The form of Hamiltonian in Eq. (3.3) is the well-known Jaynes-Cummings (JC) model [48].

### B. Coin flipping and conditional phase shift operator

In our hybrid system, the walker can be represented by the phase state of the single mode of the resonator and the coin is the two-level energy system. To implement the coin flipping operator, a microwave time-dependent driving field is applied to the circuit QED system with the form

$$\hat{H}_{\rm d} = \varepsilon(t)(a^\dagger e^{-i\omega_{\rm d}t} + a e^{i\omega_{\rm d}t}), \tag{3.4}$$

where $\omega_{\rm d}$ is the frequency of driving field. It is easy to let $\varepsilon(t)$ to be a square wave, so $\varepsilon$ is a constant when the field is turned on, while it is zero when the field is off. The Hamiltonian of the hybrid system, containing the driving field, is

$$\hat{H}_{\rm tot} = \hat{H}_{\rm JC} + \hat{H}_{\rm d}. \tag{3.5}$$

In the dispersive regime,

$$|\delta| = |\Omega - \omega_c| \gg g, \tag{3.6}$$

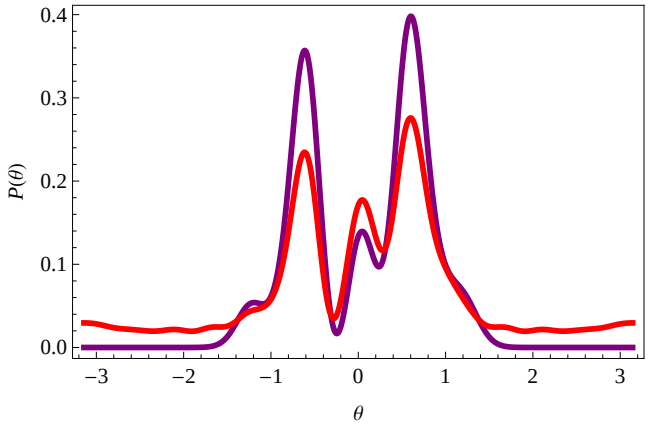


FIG. 2: (Color online.) The probability distribution of the walker in PS at the 4th step with the initial walker state $|\alpha = 3\rangle$ and coin state $(|0\rangle + i|1\rangle)/\sqrt{2}$, the step size $\Delta\theta = 0.3$, and $\varepsilon = 0.01$GHz in purple an $\varepsilon = 0.012$GHz in red respectively. The phase distribution shows a ballistic behaviour of the QW in PS. With the strength of the driving field increasing the decoherence introduced by displacement in position space increases and the phase distribution tends to be the combination of those of QW and RW.

to calculate the effective Hamiltonian from Eq. (3.5), we introduce the unitary transformation $\hat{S} = \exp[g/\delta(a\sigma_+ - a^\dagger\sigma_-)]$, and use the translated equation $\hat{S}^\dagger\hat{H}_{\rm tot}\hat{S}$ [46, 49], the Hamiltonian in Eq. (3.5) turns into the effective Hamiltonian of the whole system with driving field

$$\hat{H}_{\rm eff} = \chi a^\dagger a\sigma_z - \frac{1}{2}\delta_1\sigma_z - \delta_2 a^\dagger a + \frac{1}{2}\Omega_2\sigma_x + \varepsilon(a^\dagger + a) \tag{3.7}$$

with $\delta_1 = \omega_d - \Omega$, $\delta_2 = \omega_d - \omega_c$ , $\Omega_2 = 2g\varepsilon/\delta_2$, $\chi = g^2/\delta$.

The free evolution

$$\exp(-i\hat{H}_{\rm eff}t) \tag{3.8}$$

continues even when the driving field is off ($\varepsilon = 0$).

The evolution of the hybrid system is described by the effective Hamiltonian. The first term on the right-hand side in Eq. (3.7) contains $a^\dagger a\sigma_z$, which proves an interrelated relationship between the walker and coin, and makes the walker to evolve along clockwise or counterclockwise at the same constant angle with the orientation based on the state of the coin. The second and third terms involve the operators $\sigma_z$ and $a^\dagger a$, which represent the hence frequency of walker and the energies for the coin, respectively. The fourth term, contains $\sigma_x$, it can translate into the Hadamard coin flip by choosing a suitable pulse time. The coefficient is proportional to the Rabi frequency. The last term is the displacement in the position space and pushes the walker off the circle in PS. Thus it also causes the decoherence in the QW in PS.

## IV. NUMERICAL ANALYSIS

Now all the factors that implementation of QW needs are fulfilled. To make the the scheme working, the value of constant coefficient $\varepsilon$ in last term in Eq. (3.7) which brings the displacement in PS must be kept very small. Nevertheless, the Rabi frequency $\Omega_2$ is proportional to the pulsed driving field $\varepsilon$, so, however small $\varepsilon$ it is, we can choose a suitable pulse time to translate the $\sigma_x$ into Hadamard coin flip.

We choose the initial coin state as

$$|\varphi_0\rangle = (|0\rangle + i|1\rangle)/\sqrt{2}, \tag{4.1}$$

the initial field in the resonator as coherent state

$$|\alpha\rangle = e^{-\frac{|\alpha|^2}{2}} \sum \frac{\alpha^n}{\sqrt{n!}}|n\rangle, \tag{4.2}$$

and access to the review, realistic system parameters are [50, 51]

$$(\Omega, \omega_c, g)/2\pi = (0.7, 0.5, 0.01)\text{GHz}. \tag{4.3}$$

By choosing the coherent state $|\alpha = 3\rangle$ and different $\varepsilon$, we show the probability distribution of the walker in PS at the 4th step with step size $\Delta\theta = 0.3$ (Fig. 2). The purple line represents the circumstances with $\varepsilon = 0.01$GHz, whereas, the red line stands for the circumstances with $\varepsilon = 0.012$GHz. From Fig. 2 we see the peak probabilities with $\varepsilon = 0.012$GHz is smaller than it with $\varepsilon = 0.01$GHz because the evolution of the last term in Eq. (3.7) provides a displacement operator in position space and pushes the walker off the circle in PS. Apart from this, the rate of probability on the position $\theta = 0.01$GHz in the three main peaks with $\varepsilon = 0.012$GHz is higher than it with $\varepsilon = 0.01$GHz, that is to say, the decoherence drives the probability to the origin position, makes the distribution to Gaussian distribution. These can be regarded as the decoherence on the walker in PS and with decoherence increasing we can observe the QW-RW transmission.

In Fig. 3a, we show the ln-ln plot of the standard deviation of the probability distribution of the walker in PS with step size $\Delta\theta = 0.3$ only even steps without losing generation, the purple, red, blue, green dots represent the standard deviation of the phase distribution of QW in PS with different $\varepsilon = (0.01, 0.012, 0.015, 0.018)$GHz, respectively. With the step number increasing, the wave function of the walker meets itself on the circle in PS after 15 steps. Thus after 15 steps, the curve of the ln-ln plot of standard deviation v.s. the step number drops down. This shows difference from the QW on the line, though for the first few steps QWs on both circle and line show the ballistic behavior as expected. Overall, the slope of the points becomes small with increasing of the constant $\varepsilon$. To realize the discipline more intuitively, we cut out the standard deviation after 6, 8, and 10 steps and connect the points into line of whole circumstances (Fig. 3b). The figure shows the slopes of the line $\varsigma$ which

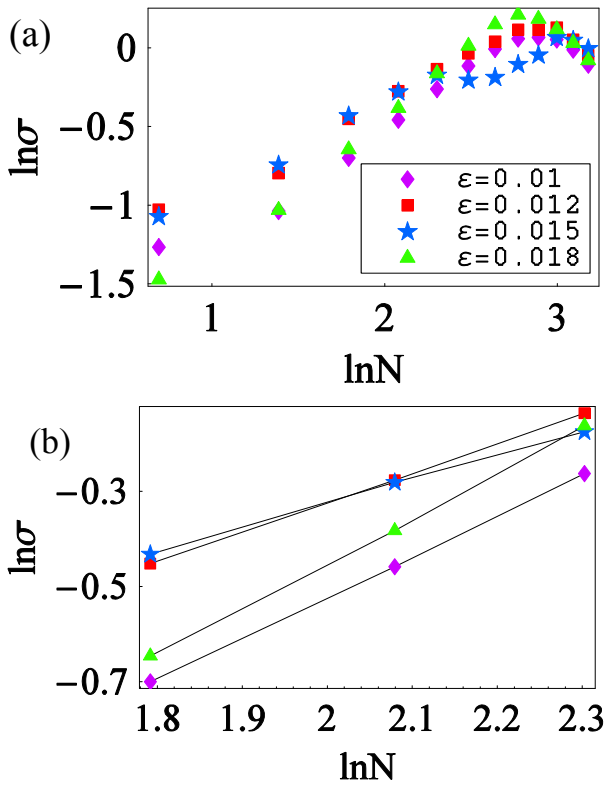


FIG. 3: (Color online.) (a) The ln-ln plot of the standard deviation of the phase distribution $\sigma$ v.s. the step number $N$ with the initial walker state $|\alpha = 3\rangle$, coin state $(|0\rangle + i|1\rangle)/\sqrt{2}$ and different strengths of the field $\varepsilon = (0.01, 0.012, 0.015, 0.018)$GHz, the step size in PS $\Delta\theta = 0.3$. The dots represent the standard deviation of even steps up to 25 steps. (b) The ln-ln plots with various $\varepsilon$ show the slopes of the plots which represent the speed of the walker spreading $\varsigma$.

is made up by the purple, red, blue, green dots are about 1, 0.89, 0.64, 0.53 respectively. Using Eq. (2.7) as a reference, the slop is 1 for QW and 0.5 for RW, different slopes of the ln-ln plots show the different behavior of the walker on circle in PS with different level of decoherence. The decoherence is introduced by the driving field which leads the walker to move in position space too. For QW in PS, it is equivalent to decoherence. With the strength of the driving field increasing the decoherence increases. Hence with decoherence increasing we see the QW-RW transition. With the increasing of the value of $\varepsilon$, the trend QW changes to RW is more obviously. So, in order to keep the more prominent properties of QW, $\varepsilon$ must be small enough.

## V. CONCLUSION

We show how a quantum walk in PS can be implemented in a quantum quincunx created through superconducting resonator-assisted quantum double dots and how interpolation from a quantum to a random walk is

implemented by controllable decoherence introduced by the displacement of the walker in position space. Our scheme shows how a QW with just one walker can be implemented in a realistic system. The coin flipping operation is implemented by driving the resonator directly, and at the same time the driving field also introduces the displacement of the walker in position space and pushes the walker off the circle in PS. Thus the displacement in position space is equivalent to decoherence on the walker in PS which is controlled by the strength of the driving field. With the strength of the driving field increasing the decoherence increases and we observe the QW-RW transition.

Although in our paper we make use of the decoherence introduced by the driving field to show the transition from QW to RW, which is one of the main points of our paper, for most of applications of QW it requires quadratic enhancement of walker spreading. The decoherence led by the driving field can be compensated with the method in [42]. The displacement of the walker in position space pushes the walker off the circle in PS by changing the mean photon number of the resonator field. Hence we can adjust the pulse duration each time according to the predicted mean photon number to compensate the effect due to the displacement and obtain a perfect QW in PS.

### Acknowledgments

This work has been supported by the National Natural Science Foundation of China under Grant No 11174052, the Open Fund from the State Key Laboratory of Precision Spectroscopy of East China Normal University. and the National Basic Research Development Program of China (973 Program) under Grant No 2011CB921203.

[1] Y. Aharonov, L. Davidovich, N. Zagury, Phys. Rev. A 48 (1993) 1687.
[2] J.K. Asbóth, Phys. Rev. B 86 (2012) 195414 .
[3] A. Wójcik, T. Luczak, P. Kurzyński, A. Grudka, T. Gdala, M. Bednarska-Bzdega, Phys. Rev. A 85 (2012) 012329.
[4] N. Konno, Quantum Information Processing 9 (2010) 405.
[5] Y. Shikano, H. Katsura, Phys. Rev. E 82 (2010) 031122.
[6] M. Genske, W. Alt, A. Steffen, A.H. Werner, R.F. Werner, D. Meschede, A. Alberti, Phys. Rev. Lett. 110 (2013) 190601.
[7] K. Manouchehri, J.B. Wang, Physical Implementation of Quantum Walks, Springer-Verlag Berlin Heidelberg 2014
[8] P.P. Rohde, J.F. Fitzsimons, A. Gilchrist, Phys. Rev. Lett. 109 (2012) 150501.
[9] T. Kitagawa, M.S. Rudner, E. Berg, E. Demler, Phys. Rev. A 82 (2010) 033429.
[10] R. Matjeschk, A. Ahlbrecht, M. Enderlein, Ch. Cedzich, A.H. Werner, M. Keyl, T. Schaetz, R.F. Werner, Phys. Rev. Lett. 109 (2012) 240503.
[11] A. Ambainis, International Journal of Quantum Information, 1 (2003) 507-518.
[12] A.M. Childs, R. Cleve, E. Deotto, E. Farhi, S. Gutmann, D.A. Spielman, Proc. 35th ACM Symposium on Theory of Computing(STOC 2003), pp. 59-68.
[13] N. Shenvi, J. Kempe, K.B. Whaley, Phys. Rev. A 67 (2003) 052307.
[14] J. Kempe, Contemporary Physics 44 (2003) 307-327.
[15] T.D. Mackay, S.D. Bartlett, L.T. Stephenson, B.C. Sanders, J. Phys. A 35 (2002) 2745-2753.
[16] T.A. Brun, H.A. Carteret, A. Ambainis, Phys. Rev. Lett. 91 (2003) 130602.
[17] P. Xue, B.C. Sanders, D. Leibfried, Phys. Rev. Lett. 103 (2009) 183602.
[18] F. Zähringer, G. Kirchmair, R. Gerritsma, E. Solano, R. Blatt, C.F. Roos, Phys. Rev. Lett. 104 (2010) 100503.
[19] H. Schmitz, R. Matjeschk, Ch. Schneider, J. Glueckert, M. Enderlein, T. Huber, T. Schaetz, Phys. Rev. Lett. 103 (2009) 090504.
[20] D. Bouwmeester, I. Marzoli, G.P. Karman, W. Schleich, J.P. Woerdman, Phys. Rev. A 61 (1999) 013410.
[21] B. Do, M.L. Stohler, S. Balasubramanian, D.S. Elliott, C. Eash, E. Fischbach, M.A. Fischbach, A. Mills, B. Zwickl, J. Opt. Soc. Am. B 22 (2005) 499.
[22] P. Zhang, X.F. Ren, X.B. Zou, B.H. Liu, Y.F. Huang, G.C. Guo, Phys. Rev. A 75 (2007) 052310.
[23] A. Peruzzo, M. Lobino, J.C.F. Matthews, N. Matsuda, A. Politi, K. Poulios, X. Zhou, Y. Lahini, N. Ismail, K. Wörhoff, Y. Bromberg, Y. Silberberg, M.G. Thompson, J.L.O'Brien, Science 329 (2010) 1500.
[24] H.B. Perets, Y. Lahini, F. Pozzi, M. Sorel, R. Morandotti, Y. Silberberg, Phys. Rev. Lett. 100 (2008) 170506.
[25] L. Sansoni, F. Sciarrino, G. Vallone, P. Mataloni, A. Crespi, R. Ramponi, R. Osellame, Phys. Rev. Lett. 108 (2012) 010502.
[26] Y.C. Jeong, C. Di Franco, H.T. Lim, M.S. Kim, Y.H. Kim, Nature Communication 4 (2013) 2471.
[27] M.A. Broome, A. Fedrizzi, B.P. Lanyon, I. Kassal, A. Aspuru-Guzik, A.G. White, Phys. Rev. Lett. 104 (2010) 153602.
[28] P. Xue, H. Qin, B. Tang, B.C. Sanders, New J. Phys. 16 (2014) 053009.
[29] A. Schreiber, K.N. Cassemiro, V. Potoček, A.Gábris, P.J. Mosley, E. Andersson, I. Jex, C. Silberhorn, Science 336 (2012) 55.
[30] P. Xue, H. Qin, B. Tang, Scientific Reports, 4 (2014) 4825.
[31] H.W. Chen, X. Kong, B. Chong, G. Qin, X.Y. Zhou, X.H. Peng, J.F. Du, Phys. Rev. A 83 (2011) 032314.
[32] M.S. Kuznetsova, K. Flisinski, I. Ya. Gerlovin, M.Yu. Petrov, I.V. Ignatiev, S.Yu. Verbin, D.R. Yakovlev, D. Reuter, A.D. Wieck, M. Bayer, Phys. Rev. B 89 (2014) 125304.
[33] D. Culcer, A.L. Saraiva, B. Koiller, X.D. Hu, S. D. Sarma, Phys. Rev. Lett. 108(2012) 126804.
[34] H.P. Paudel, M.N. Leuenberger, Phys. Rev. B 88 (2013) 085316.

[35] J.R. Petta, A.C. Johnson, J.M. Taylor, E.A. Laird, A. Yacoby, M.D. Lukin, C.M. Marcus, M.P. Hanson, A.C. Gossard, Science 309 (2005) 2180.
[36] A.C. Johnson, Nature 435 (2005) 925.
[37] D. Solenov, S.E. Economou, T.L. Reinecke, Phys. Rev. B 87(2013) 035308.
[38] G. Burkard, A. Imamoglu, Phys. Rev. B 74 (2006) 041307(R).
[39] Z.R. Lin, G.P. Guo, T. Tu, F.Y. Zhu, G.C. Guo, Phys. Rev. Lett. 101(2008) 230501.
[40] V.N. Golovach, M. Borhani, D. Loss, Phys. Rev. A 81 (2010) 022315.
[41] Z. Burda, J. Duda, J.M. Luck, B. Waclaw, Phys. Rev. Lett. 102 (2009) 160602.
[42] P. Xue, B.C. Sanders, A. Blais, K. Lalumiére, Phys. Rev. A 78 (2008) 042334.
[43] P. Xue, B.C. Sanders, Phys. Rev. A 87 (2013) 022334.
[44] B.C. Sanders, S.D. Bartlett, B. Tregenna, P.L. Knight, Phys. Rev. A 67 (2003) 042305.
[45] J.M. Taylor, H.A. Engel, W. D¨r, A. Yacoby, C.M. Marcus, P. Zoller, M.D. Lukin, Nature Physics 1 (2005) 177-183.
[46] A. Blais, R.S. Huang, A. Wallra , S.M. Girvin, R.J. Schoelkopf, Phys. Rev. A 69 (2004) 062320.
[47] R. Schoelkopf, A. Clerk, S. Girvin, K. Lehnert, M. Devoret, Kluwer Academic, Dordrecht (2003) Chap. 9, pp. 175-203.
[48] E.T. Jaynes, F.W. Cummings, Proc. IEEE 51 (1963) 89.
[49] D.F. James, J. Jerke, Canadian J. Phys. 85 (2007) 625.
[50] D.I. Schuster, A.A. Houck, J.A. Schreier, A. Wallraff, J.M.Gambetta, A. Blais, L.Frunzio, J. Majer, B. Johnson, M.H.Devoret, S.M. Girvin, R.J. Schoelkopf, Nature 445 (2007) 515.
[51] A. Blais, J. Gambetta, A. Wallraff, D.I. Schuster, S.M. Girvin, M.H. Devoret, R.J. Schoelkopf, Phys. Rev. A 75 (2007) 032329.